

Supplementary Video 1 Imaging of a human stool sample, supplemented with *Human rotavirus*, with the LVEM25 in STEM mode (15 kV). Negative staining with 0.5% UA. The video sequence zooms in real-time on a single rotavirus particle which is attached to the cell wall of a bacterium. At the end of the sequence scanning speed is reduced (increase of filter number) to improve resolution.

Supplementary Figure 1. Negative staining of Tobacco mosaic virus (TMV) with 1% UA. The central channel (width = 4 nm) of the filamentous capsid (arrows) was visible with all microscopes used in this study. In contrast, the layer lines of the capsid are clearly visible only with the high-voltage TEM (HV TEM) (arrowheads). A Low-voltage TEM (LV TEM; LVEM25). B SEM (TeneoVS) using the STEM3+ detector in bright-field mode. C High-voltage TEM (HV TEM; JEM-2100). Scale bars = 50 nm. Figure A was recorded by Eva Coufalova at the headquarters of DeLong Instruments in Brno.

Supplementary Figure 2. Imaging of stained and unstained ultrathin sections through C6/36 insect cells, infected with *Culex theileri* flavivirus, using the LVEM25 at 25 kV. Sections were collected on naked grids and coated with carbon. Images were not corrected for contrast/brightness and left unfiltered. Groups of viruses within the dilated endoplasmic reticulum are shown at three different magnifications. Images from stained and unstained sections show no significant difference in contrast/brightness or other aspects of image quality. Scale bars in A, B = 1 μ m and C, D = 200 nm and in E, F = 200 nm.

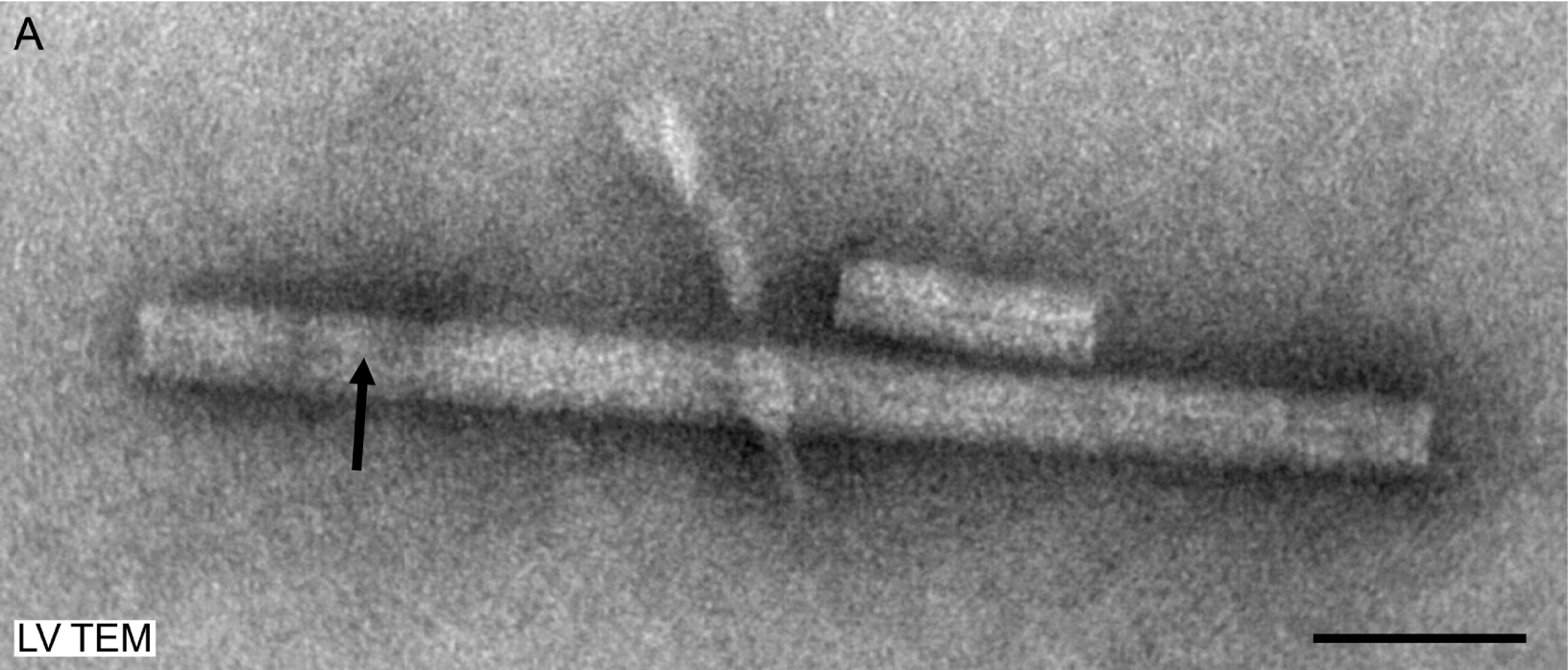
Supplementary Figure 3. Imaging of stained and unstained ultrathin sections through C6/36 insect cells, infected with *Culex theileri* flavivirus, using the SEM in STEM mode at 30 kV. Sections were collected on naked grids and coated with carbon. Images were not corrected for contrast/brightness and left unfiltered. Groups of viruses within the dilated endoplasmic reticulum are shown at three different magnifications. Images from stained and unstained sections allow recognition of ultrastructural detail at all magnifications. However, to find optimal contrast settings for the STEM detector was difficult with unstained sections and at higher magnification image contrast was significantly lower with unstained sections than with stained sections. Scale bars in A, B = 1 μ m and C, D = 200 nm and in E, F = 200 nm.

Supplementary Figure 4. Imaging of stained and unstained ultrathin sections through C6/36 insect cells, infected with *Culex theileri* flavivirus, using the HV TEM at 200 kV. Sections were collected on naked grids and coated with carbon. Images were not corrected for contrast/brightness and left unfiltered. Groups of viruses within the dilated endoplasmic reticulum are shown at three different magnifications. Images from stained and unstained sections allow recognition of ultrastructural detail at all magnifications. However, image contrast was much lower with unstained sections. Scale bars in A, B = 1 μ m and C, D = 200 nm and in E, F = 200 nm.

Supplementary Figure 5. Scan traces (arrows) left by STEM-imaging with the SEM at higher magnification. A Negative staining (0.5% UA) of a stool sample supplemented with Human rotavirus. B Thin section of *Acanthamoeba polyphaga* mimivirus on naked grids (with section staining and carbon coating). Bars = 200 nm.

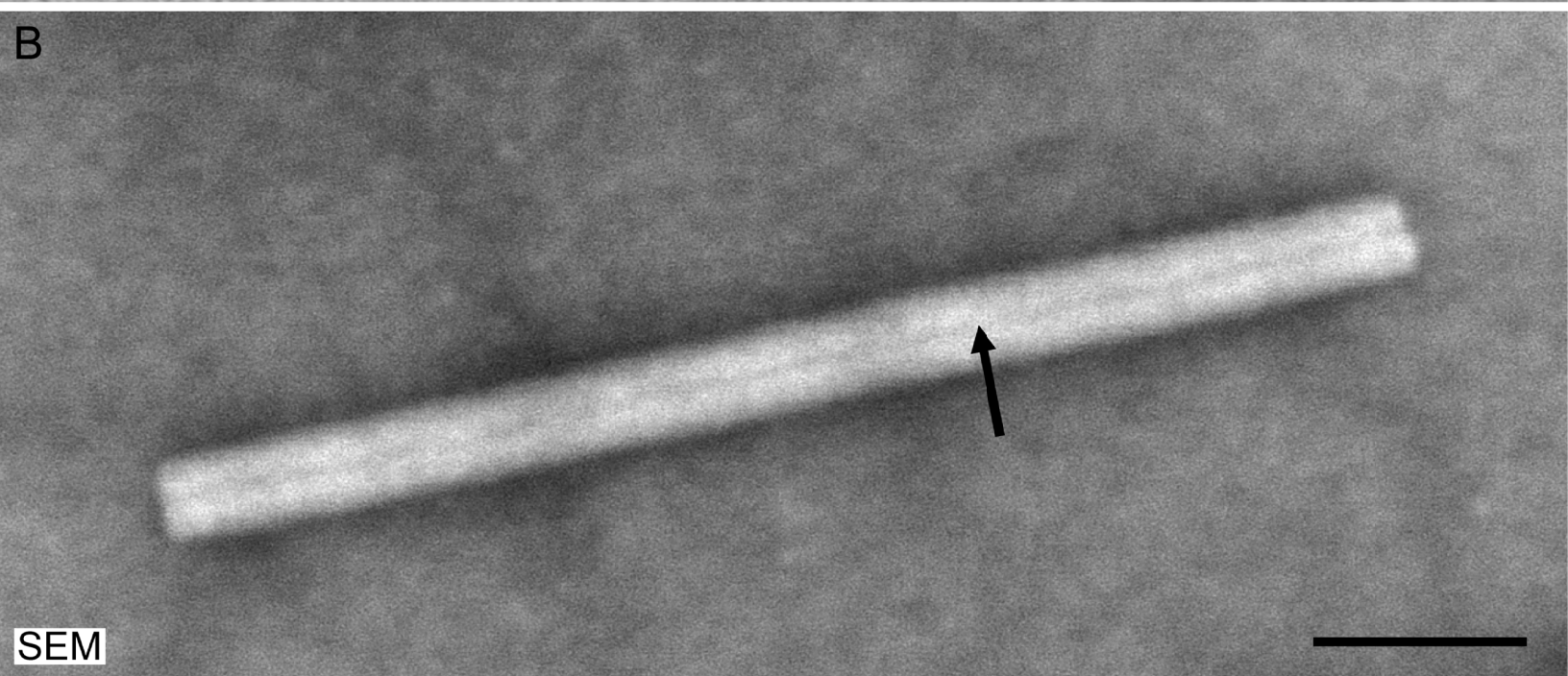
Supplementary Figure 6. Images from blinded virus recognition testing using the STEM mode of the SEM (images were adjusted for brightness and contrast but not filtered). A Influenza A virus A/X-31(H3N2), 0.5% PTA (sample code: EQA32-1). B Infectious pancreatic necrosis virus (Birnaviridae), 1% PTA (sample code EQA31-5). C Sandfly fever Naples phlebovirus, 0.5% PTA (sample code: EQA 32-2). D Chikungunya virus, 0.5% UA (sample code: EQA 32-6). E Feline calicivirus, 1% UA (sample code: EQA 32-5). F Orf virus (Poxviridae), 1% PTA (sample code: EQA 31-2).

A



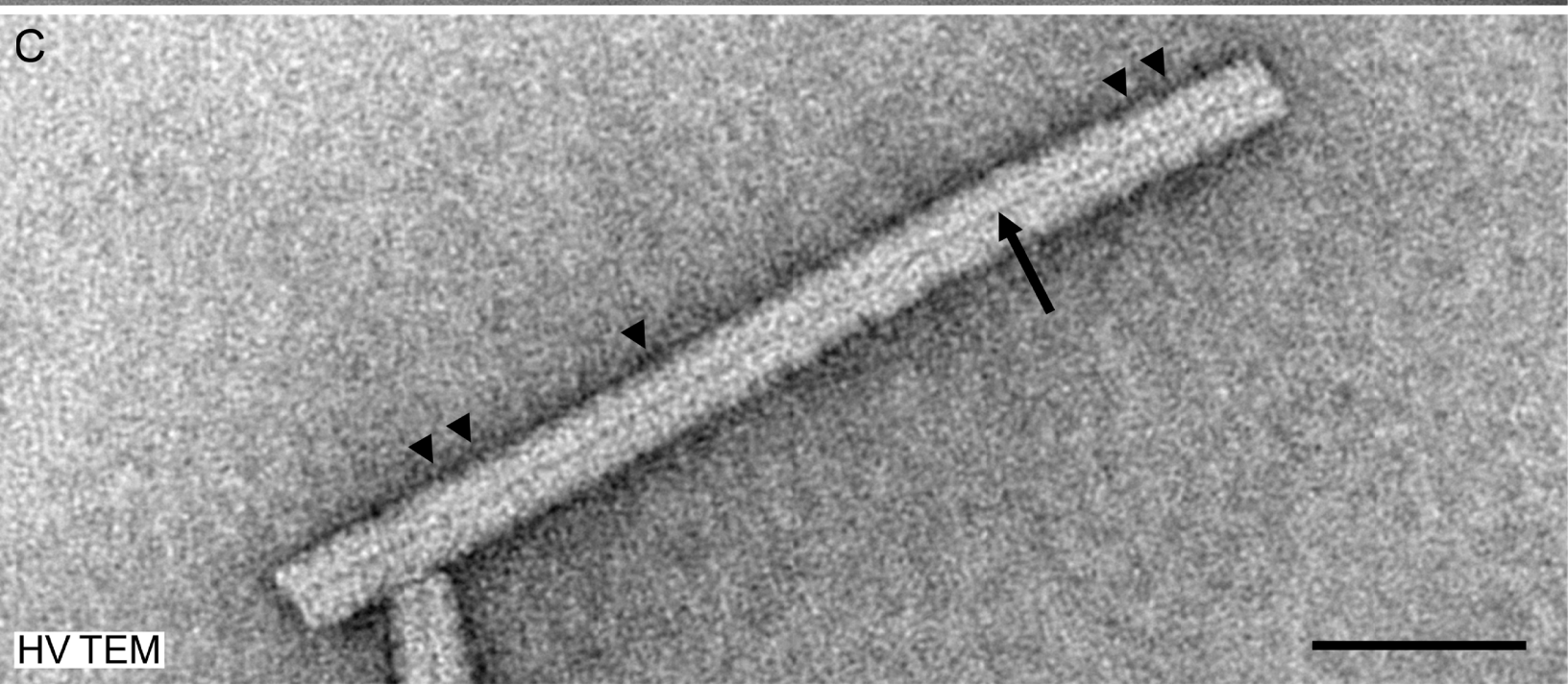
LV TEM

B



SEM

C



HV TEM

